Comprehensive Quantification of Signal-to-Noise Ratio and *g*-Factor for Image-Based and *k*-Space-Based Parallel Imaging Reconstructions

Philip M. Robson,[1*] Aaron K. Grant,[1] Ananth J. Madhuranthakam,[2] Riccardo Lattanzi,[1,3] Daniel K. Sodickson,[4] and Charles A. McKenzie[5]

Parallel imaging reconstructions result in spatially varying noise amplification characterized by the *g*-factor, precluding conventional measurements of noise from the final image. A simple Monte Carlo based method is proposed for all linear image reconstruction algorithms, which allows measurement of signal-to-noise ratio and *g*-factor and is demonstrated for SENSE and GRAPPA reconstructions for accelerated acquisitions that have not previously been amenable to such assessment. Only a simple "prescan" measurement of noise amplitude and correlation in the phased-array receiver, and a single accelerated image acquisition are required, allowing robust assessment of signal-to-noise ratio and *g*-factor. The "pseudo multiple replica" method has been rigorously validated in phantoms and in vivo, showing excellent agreement with true multiple replica and analytical methods. This method is universally applicable to the parallel imaging reconstruction techniques used in clinical applications and will allow pixel-by-pixel image noise measurements for all parallel imaging strategies, allowing quantitative comparison between arbitrary *k*-space trajectories, image reconstruction, or noise conditioning techniques. Magn Reson Med 60:895–907, 2008. © 2008 Wiley-Liss, Inc.

Key words: signal-to-noise ratio; image noise; *g*-factor; parallel imaging; image reconstruction

Parallel imaging approaches are widely used for accelerating MR image acquisitions (Simultaneous Acquisition of Spatial Harmonics (SMASH) (1), Sensitivity Encoding (SENSE) (2), Generalized Auto-Calibrating Partially Parallel Acquisition (GRAPPA) (3). Receiving signals simultaneously in the independent elements of a radiofrequency coil array allows acquisition of some of the phase-encoded signals to be omitted. The distinct spatial sensitivity profiles of the elements contain spatial information that may be used for the purpose of spatial encoding in the image that is normally provided by application of magnetic field gradients. The penalty for acquiring fewer signals is a loss of Signal-to-Noise Ratio (SNR) in the final image by a factor of the square root of the acceleration factor $\sqrt{R}$ due to reduced signal averaging. In parallel imaging image-noise is further amplified by the ill-conditioning of the image reconstruction process. In general, the noise amplification is spatially variant and depends on the specific geometry of the radiofrequency coil array used and is therefore characterized by the (geometry) *g*-factor (2). An accurate and quantitative method of analyzing noise amplification is essential for objective comparison between parallel imaging techniques and between image reconstruction methods when developing new methods and designing clinical imaging protocols. Spatial variation of the image noise precludes the conventional (and simple) Region-of-Interest (ROI) approach for SNR estimation which uses a region of signal within the object and a region of noise outside of the object (4,5), making SNR difficult to deal with practically in parallel imaging. Quantification of noise amplification in parallel imaging has been studied previously (2,6), producing methods for direct calculation of image noise, *g*-factor (2) and SNR (7) for some classes of parallel imaging strategies. However, all existing techniques are subject to certain regimes in which it is impossible to calculate SNR analytically. Direct image noise matrix approaches (2) require memory for matrices of size $O(n^2)$, where n may be as large as N^2 for arbitrary *k*-space trajectories and generalized SENSE image reconstruction (8), where N is the image matrix dimension. Typically N may be 256, which, for complex floating-point data, leads to a reconstruction matrix of approximately 30 Gb. For direct GRAPPA approaches n may be as large as N^3 (9) leading to a reconstruction matrix of approximately 2000 Tb. Furthermore, matrix inversion approaches require $O(n^3)$ operations (8). Thus, direct computation rapidly may become intractable such that currently there is no universal approach for measuring SNR or *g*-factor.

Statistical methods, for example Monte Carlo and bootstrapping methods (10), are often used in functional parameter estimation from MRI (e.g., Jones and Steger et al.) (11,12). This work develops a simple Monte Carlo method for rigorously calculating image noise propagating through the image reconstruction itself (similarly to methods explored previously) (13,14). This method allows calculation of SNR and *g*-factor for all parallel imaging techniques which use a linear image reconstruction algorithm, irrespective of whether direct calculation is available or computationally tractable. In this work we demonstrate noise analysis for two classes of parallel imaging methods (SENSE and GRAPPA) routinely used in clinical imaging applications.

[1]Department of Radiology, Beth Israel Deaconess Medical Center, Boston, Massachusetts.

[2]Global Applied Science Lab., GE Healthcare, Boston, Massachusetts.

[3]Harvard-MIT Division of Health Sciences and Technology, Boston, Massachusetts.

[4]Department of Radiology, New York University School of Medicine, New York, New York.

[5]Department of Medical Biophysics, The University of Western Ontario, London, Ontario, Canada.

*Correspondence to: Philip M. Robson, Beth Israel Deaconess Medical Center, Department of Radiology, Room, Ansin 242, 330 Brookline Avenue, Boston, MA 02215. E-mail: probson@bidmc.harvard.edu

Received 30 October 2007; revised 7 April 2008; accepted 15 May 2008.

DOI 10.1002/mrm.21728

Published online in Wiley InterScience (www.interscience.wiley.com).

IMAGE NOISE ANALYSIS FOR LINEAR RECONSTRUCTION ALGORITHMS

As described by Pruessmann et al. (2), for a linear image reconstruction the propagation of noise from the sampled values in *k*-space into the image noise is described by noise matrices. The image reconstruction is described by the operation of the reconstruction matrix **F** on the vector of *k*-space data **s**, to generate image pixel values in the vector **ρ** (Eq. [1]).

$$\boldsymbol{\rho} = \mathbf{F}\mathbf{s} \quad [1]$$

The variance of the pixel values in the p^{th} element of **ρ** is given by the p^{th} diagonal entry in the image noise matrix **X**.

$$\mathbf{X} = \mathbf{F}\tilde{\boldsymbol{\Psi}}\mathbf{F}^{\dagger} \quad [2]$$

The sample noise matrix $\tilde{\boldsymbol{\Psi}}$ (2) is the Kronecker product of the noise covariance matrix **Ψ** and an identity matrix of dimension N_{acq} equal to the number of acquired *k*-space points (the length of vector **s** divided by the number of coil elements) (Eq. [3]).

$$\tilde{\boldsymbol{\Psi}} = \boldsymbol{\Psi} \otimes \mathbf{I}_{Nacq} \quad [3]$$

The noise covariance matrix describes the level and correlation of noise in the signals received in each element of the coil array. The noise covariance matrix may be expressed in terms of the individual noise records n_{ik} (noise samples $1 \leq k \leq N_k$ for coil *i*) received in each coil element in the absence of NMR signal (Eq. [4], where * represents complex conjugation) (7).

$$\Psi_{ij} = \frac{1}{2N_k} \sum_{k=1}^{N_k} n_{ik} n_{jk}^{*} \quad [4]$$

Trivially, a conventional Fourier Transform image reconstruction is a linear operation that may be expressed in the matrix form of Equation [1]. Noise amplification may also be characterized analytically using this formalism. The *g*-factor is simply the ratio of the SNR for an optimal unaccelerated image and the SNR of the accelerated image with an additional factor of the acceleration factor *R* which accounts for the SNR loss due to averaging fewer acquired signals (Eq. [5]).

$$g = \frac{\text{SNR}_{\text{optimal,unaccelerated}}}{\text{SNR}_{\text{accelerated}} \cdot \sqrt{R}} = \frac{\text{SD}_{\text{accelerated}}}{\text{SD}_{\text{optimal,unaccelerated}} \cdot \sqrt{R}} \quad [5]$$

Equivalently, assuming the image signal is the same in the accelerated and unaccelerated optimal reconstructions (which is explicitly required by the formalism of the SENSE reconstruction in Pruessmann et al.) (2) the *g*-factor may be expressed in terms of the image noise standard deviations (SD) leading to the familiar expression of *g*-factor in terms of image noise matrix terms (Eq. [6]).

$$g_p = \frac{\sqrt{\text{X}_{pp}^{\text{accelerated}}}}{\sqrt{R \cdot \text{X}_{pp}^{\text{optimal,unaccelerated}}}} \quad [6]$$

The optimal SNR image is achieved by considering the noise correlations between elements of the coil array as described by Roemer et al. (15). Therefore, it follows that an unaccelerated image reconstruction may be suboptimal and may by our current definition have a *g*-factor greater than unity.

This analytical approach allows image reconstructions to include "division by the image noise" to generate pixel values in units of SNR, whereby the normal image pixel is divided by the calculated image noise for that pixel (hereafter referred to as the "direct SNR method"). Kellman and McVeigh (7) describe image reconstructions in SNR-units by the direct SNR method for fully gradient-encoded (unaccelerated) acquisitions and accelerated acquisitions using a SENSE technique. The direct method provides an image with pixel-by-pixel SNR values which faithfully represent the spatial variation in image noise resulting from parallel imaging acquisition to complement the information in the conventional magnitude image.

Most clinical applications of parallel imaging follow either the SENSE or the GRAPPA approaches. SENSE image reconstructions may be generalized (2,8,16) as a pseudo-inverse of the encoding matrix **E** which expresses the *k*-space signals received by each element of a coil array receiver **s** as the Fourier transform of the object **ρ** multiplied by the complex spatial sensitivity of the coil element (Eqs. [7] and [8]).

$$\mathbf{s} = \mathbf{E}\boldsymbol{\rho} \quad [7]$$

$$\boldsymbol{\rho} = (\mathbf{E}^{\dagger}\tilde{\boldsymbol{\Psi}}^{-1}\mathbf{E})^{-1}\mathbf{E}^{\dagger}\tilde{\boldsymbol{\Psi}}^{-1}\mathbf{s} \quad [8]$$

It can be seen in Equation [8] that all generalized SENSE image reconstructions obey the linear formulation required in Equation [1] for the analytical image noise matrix formalism of Equation [2] to hold.

GRAPPA techniques reconstruct missing phase-encoded lines in *k*-space by linearly combining neighboring lines. The weighting factors for the combination are determined from fitting lines to a small additional number of autocalibration signal (ACS) lines acquired around the center of *k*-space. This is a generalization of similar *k*-space fitting approaches (1,17). In other techniques, for example, AUTO-SMASH (17), the linear combination of *k*-space lines produces a single composite *k*-space from which a final image is reconstructed by Fourier transform. As described by Griswold et al. (3), the GRAPPA approach reconstructs fully sampled *k*-space data for each element of the coil array before reconstructing an image for each coil by Fourier transform and enjoys the SNR advantage of a root-sum-of-squares (RSS) combination of the separate coil images.

The RSS step, specifically intended to improve SNR (and avoid phase cancellation problems), is nonlinear and precludes use of the image noise matrix formalism to calculate image noise and *g*-factor directly. This has proven an obstacle to detailed analysis of the characteristics of noise propagation in the GRAPPA method beyond appreciating the excellent appearance of various images reconstructed by the GRAPPA method. However, the RSS coil-combination is a simplification of the full complex coil

combination described by Roemer et al. (15) for the unaccelerated case. Use of complex combinations allows the GRAPPA reconstruction to be written as a linear matrix operation (9). In this alternative formulation, each of the steps of the GRAPPA reconstruction may be expressed as a matrix operation. First, missing phase-encoded lines in the undersampled *k*-space are reconstructed by the operation of a transfer matrix **T**, which performs linear combinations of neighboring lines. Second, a Fourier transform matrix **H** is applied to the now repleted *k*-space data matrix from each coil. Finally, a complex coil-combination matrix $\hat{\mathbf{C}}$ (9) is applied to form the vector of final image pixels $\boldsymbol{\rho}$ (Eq. [9]).

$$\boldsymbol{\rho} = \hat{\mathbf{C}}\mathbf{H}\mathbf{T}\mathbf{s} \quad [9]$$

Complex coil combination allows the GRAPPA reconstruction to be expressed as a linear operation and, therefore, noise propagation may be analyzed using the image noise formalism of Eq. [2]. The coil sensitivities used in the matrix $\hat{\mathbf{C}}$ may be calculated from a separate image or from the central lines of the acquired *k*-space data in a "self-calibrating" approach. The linear matrix representation "complex-GRAPPA" approach is discussed in Robson et al. (9).

Limitations of Conventional Noise Analysis

The formality of writing the reconstruction in a matrix operation form for the purpose of noise analysis carries the high computational burden of handling many data at once. The size of the reconstruction matrix for SENSE and GRAPPA methods with 1-D acceleration is $O(N_y \text{ by } N_{ky} \times c)$, where N_y and N_{ky} are the number of data in the image- and *k*-space y-dimension, and c is the number of coil elements. The computation for the generalized SENSE method is more demanding as this involves inversion of a matrix of this order of magnitude (8). In volumetric image acquisitions where acceleration is applied in two dimensions, which is commonly the case in clinical applications, the matrices become larger, $O(N_y \times N_z \text{ by } N_{ky} \times N_{kz} \times c)$, where N_z and N_{kz} are equivalent quantities in the z-dimension; furthermore, in GRAPPA methods where the reconstruction kernel may span three dimensions (18), the matrix expands into a further dimension leading to a reconstruction matrix size $O(N_x \times N_y \times N_z \text{ by } N_{kx} \times N_{ky} \times N_{kz} \times c)$. Thus direct calculation of SNR and *g*-factor by means of image noise matrices soon becomes computationally intractable. It should be noted that 2D-Cartesian-SENSE (19) is computationally tractable because the regularly undersampled data permit contraction of the generalized matrix expression into small sub-blocks. For variable density *k*-space sampling schemes coupled with 2D acceleration, the full matrix must be used. Non-Cartesian *k*-space sampling trajectories, including radial and spiral techniques, where it is not possible to form discrete sets of aliased pixels are another important class of image acquisitions for which an analytical and computationally tractable matrix reconstruction may not be available due to the size of the reconstruction matrix. In all such cases where the matrix approach of image reconstruction is not feasible an alternative approach is used. For SENSE techniques, an iterative conjugate-gradient (CG) technique may be applied to reconstruct the image as described in Pruessmann et al. (8). For GRAPPA techniques, many small convolution operations are applied to the undersampled *k*-space followed by a standard Fourier Transform algorithm (indeed this is the conventional implementation of the GRAPPA reconstruction for Cartesian sampling, and with additional regridding of the data for non-Cartesian GRAPPA) (20). However, direct calculation of the image noise and *g*-factor is not possible without forming the reconstruction matrix; indeed iterative approaches for generalized SENSE do not yield explicitly the reconstruction weights which form the reconstruction matrix.

Direct calculation of image noise becomes intractable whenever the reconstruction matrix becomes too large to be computationally feasible, including the following: (i) Cartesian SENSE with variable density *k*-space traversal and 2D acceleration; (ii) Generalized SENSE with arbitrary *k*-space trajectories (e.g., spirals); (iii) GRAPPA with 2D acceleration (including regular undersampling schemes); (iv) GRAPPA with 2D or 3D reconstruction kernels.

A PSEUDO MULTIPLE REPLICA APPROACH

As an alternative to the analytical matrix-based approach, image noise amplifications may be determined from the variations in image pixel values caused by random noise fluctuations in the input *k*-space signals where the image reconstruction is considered to be a "black-box" signal processing block.

The gold-standard image noise measurement is the so-called "actual multiple replica" method where *k*-space signals are acquired multiple times and reconstructed using the same "black-box" into a stack of equivalent image replicas which differ only in their noise content. Image noise may then be found on a pixel-by-pixel basis by finding the standard deviation of pixel values through the stack of image replicas. Acquisition of multiple image replicas allows assessment of image noise and thus SNR on a pixel-by-pixel basis and is therefore useful for measuring the spatially-variant amplified noise in parallel imaging (4,5). The use of this gold standard is not feasible in practice for "real-world" in vivo imaging due to excessive patient motion or physiologic noise between image acquisitions, susceptibility to instrument drift (21), and prolonged examination times.

For a linear "black-box" signal processing block the image noise is solely dependent on the noise in the signal and the reconstruction can be seen to operate on the image and the noise separately. We propose a simple Monte Carlo technique hereafter termed the "pseudo multiple replica method" for obtaining a robust measurement of image noise for all linear image reconstructions which may be used when a direct calculation is not possible. Correctly scaled and correlated synthetic random noise is added to the acquired *k*-space before "black-box" image reconstruction. This process is repeated multiple times, each time with different synthetic noise, to produce a stack of independent image replicas from which image noise may be calculated emulating the gold-standard actual multiple replica method. A previous study (13) has used this approach with synthetic Gaussian noise without consider-

ing noise correlations. Another study (14) applied a bootstrap method, reordering acquired noise, to estimate the noise propagation through the image reconstruction that included noise correlations and scaling without needing to generate "fresh" noise for each replica. The pseudo multiple replica method is based on prior knowledge of the signal noise in *k*-space. It does not require explicit knowledge of the reconstruction matrix and requires acquisition of *k*-space only once to calculate SNR of the accelerated image.

The iterative conjugate gradient method for SENSE methods is linear and thus may be used with the pseudo multiple replica method. For GRAPPA methods, the conventional image reconstruction which applies many small convolutions before RSS coil-combination is nonlinear only in the final RSS step. Therefore, a linear complex-GRAPPA may be implemented in both a full matrix form (transfer matrix used to reconstruct *k*-space) and the conventional form of reconstruction. Thus a linear conventional GRAPPA technique may be used with the pseudo multiple replica method. ("RSS-GRAPPA" will be specified explicitly hereafter, with "conventional" referring to *k*-space reconstruction and "complex" referring to complex coil combination.).

THEORY

Pseudo Multiple Replica Method

On the assumption that repeatedly acquired *k*-space data differs only in its noise content, the signal component being unchanged, synthetic complex noise, correctly scaled and correlated between elements of the coil array, may be added to *k*-space to emulate actual multiple replica acquisition before image reconstruction (see Fig. 1). Noise may be added uniformly to *k*-space; the characteristic spatial variance of noise occurs only in image space after image reconstruction. The pseudo multiple replica method takes advantage of the linearity of the image reconstruction. Each pseudo replica image has the correct representation of the image noise despite being noisier than the original acquired image by a factor of $\sqrt{2}$ after

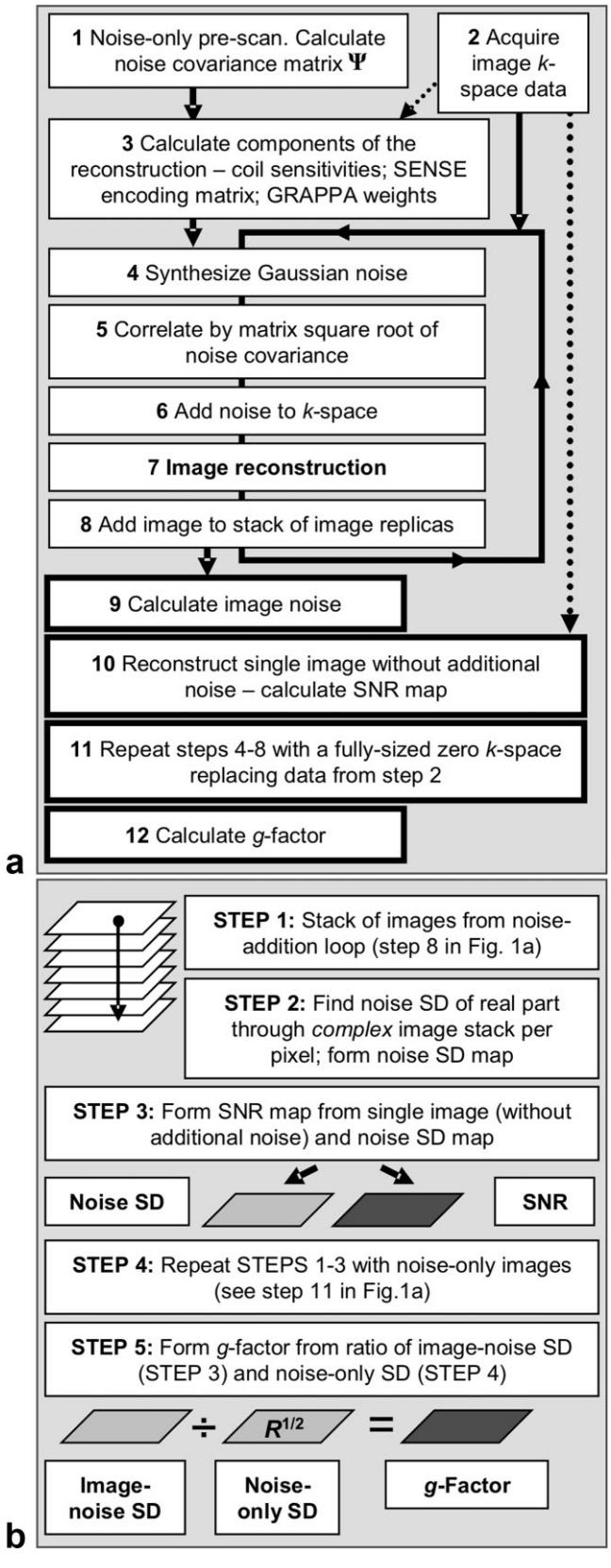

FIG. 1. **a:** The pseudo multiple replica method. Image *k*-space and the noise prescan data are acquired once (steps 1–3). The noise covariance matrix is used to scale and correlate unity SD Gaussian noise for every replica loop (steps 4–7). The reconstructed image is added to a stack of replicas before repeating the noise-addition loop (step 8). For self-calibrated techniques, the reconstruction matrix is calculated from the original data and is used for all replicas. The stack of replicas is then used to calculate SNR (step 9–10). In step 11, the multiple replica loop is repeated using an artificial fully-sized zero *k*-space to analyze noise from an un-accelerated acquisition and with an image reconstruction that is simply an FFT and an optimal complex coil combination. Finally, *g*-factor is calculated (step 12). **b:** The steps involved in forming the SNR and *g*-factor for both SENSE and GRAPPA image reconstructions. Noise SD is found from the standard deviation of the real or imaginary parts of the complex pixel values for each pixel location through the stack of replicas (STEP 2). In STEP 5, the *g*-factor is found from the two noise SD maps divided by the square root of the acceleration factor *R*.

addition of the second independent set of pseudo noise data. The actual image noise, which cannot be removed from the acquired *k*-space, remains in every image replica and appears as part of the "true" image when the image noise is calculated from the stack of pseudo image replicas. The noise is found from the standard deviation of either the real or imaginary components of the complex image pixel values through the stack of replicas because the linear reconstruction transforms noise in an equivalent manner in either component of the complex signal. As many replicas as desired for calculating standard deviation may be formed.

Linearity of an image reconstruction also ensures that Gaussian distributed white noise in the received NMR signal is transformed into Gaussian noise in the image domain. Thus, the standard deviation of image pixel values takes an intuitive interpretation defining the range in which the true pixel value may be found, or, equivalently, the amount by which the pixel value may vary due to random noise fluctuations alone. Furthermore, linear reconstructions do not suffer from noise biasing which results from magnitude operations (7,22).

Scaling and correlation of the noise is determined from the signal acquired during a "noise prescan" when the receiver is opened with no RF pulses and no normal MR signal present, as described by Kellman and McVeigh (7) (see Fig. 1a). The coils must be loaded as for imaging so that the noise received is that originating from the object; and the coil must be in place as for imaging so that the noise correlations due to coupling of component coils are correctly measured. The bandwidth of the receiver and the receiver gains are set as for imaging to ensure the noise is scaled correctly. Further details of the noise prescan may be found in Kellman and McVeigh (7).

The noise covariance matrix Ψ_{ij} measuring the noise level (diagonal elements) and correlation (off-diagonal elements) between coils *i* and *j* (where *i* and *j* run from 1 to the number of coils, *c*) in the coil array may be formed (7,23) from the measured noise prescan data according to Equation [10] with the noise records n_{ik} of *N* complex points sampled at time intervals indexed by *k* from the i^{th} component coil.

$$\Psi_{ij} = \frac{1}{2N}\sum_{k=1}^{N} n_{ik} n_{jk}^{*} \qquad [10]$$

Scaled and correlated noise records for each channel *i* of the phased-array n_{ik}^{corr} are formulated from uncorrelated Gaussian-distributed white noise n_{ik}^{G} with unity standard deviation by matrix multiplication with the principal matrix square root of the measured noise covariance matrix (Eq. [11]) such that the noise covariance matrix is recovered upon multiplication of correlated noise records (Eq. [12]), given that the principal square root of the noise covariance matrix is equal to its Hermitian conjugate.

$$n_{ik}^{corr} = \sum_{j=1}^{c} \Psi_{ij}^{1/2} n_{jk}^{G} \qquad [11]$$

$$\frac{1}{2N}\sum_{k=1}^{N} n_{ik}^{corr} n_{jk}^{corr*} = \frac{1}{2N}\sum_{k=1}^{N}\left(\sum_{p=1}^{c}\Psi_{ip}^{1/2} n_{pk}^{G}\sum_{q=1}^{c}\Psi_{jq}^{1/2*} n_{qk}^{G*}\right)$$

$$= \frac{1}{2N}\sum_{p=1}^{c}\sum_{q=1}^{c}\Psi_{ip}^{1/2}\Psi_{jq}^{1/2*}\sum_{k=1}^{N} n_{pk}^{G} n_{qk}^{G*}$$

$$= \frac{1}{2N}\sum_{p=1}^{c}\sum_{q=1}^{c}\Psi_{ip}^{1/2}\Psi_{jp}^{1/2*} 2N\delta_{pq} = \sum_{p=1}^{c}\Psi_{ip}^{1/2}\Psi_{pj}^{1/2} = \Psi_{ij} \qquad [12]$$

The matrix square root $\Psi_{ij}^{1/2}$ is given by the matrix of eigenvectors V_{ij} and the diagonal matrix of square roots of eigenvalues S_{pq}

$$\Psi_{ij}^{1/2} = \sum_{p=1}^{c}\sum_{q=1}^{c} V_{ip} S_{pq} V_{qj}^{-1} \qquad [13]$$

from the eigen-decomposition of the noise covariance matrix Ψ_{ij}

$$\Psi_{ij} = \sum_{p=1}^{c}\sum_{q=1}^{c} V_{ip} D_{pq} V_{qj}^{-1} \qquad [14]$$

where D_{pq} is the diagonal matrix of eigenvalues. The principal matrix square root is given by taking all positive square roots of the eigenvalues. For the Hermitian-positive definite noise covariance matrix, all eigenvalues are real and positive, and the eigenvectors form a unitary basis, so that it can be seen that $\Psi_{ij}^{1/2}$ is equal to its Hermitian conjugate as required in Equation [12]. The *principal* matrix square root of the noise covariance matrix was chosen arbitrarily as the "correlating matrix." The Cholesky decomposition of the noise covariance matrix into a lower triangular matrix L_{ij} and its Hermitian conjugate is an equivalent choice for the correlating matrix as previously used by Pruessmann et al. (8). To confirm the freedom of choice Gaussian noise was correlated with the principal matrix square root, another of the matrix square roots from the eigen-decomposition, and the lower triangular matrix from the Cholesky decomposition. The noise SD of each of the correlated channels was found to be the same for each method used. Thus, any appropriate choice of the correlating matrix produces equivalent results when used with the pseudo multiple replica method.

SNR Maps From the Pseudo Multiple Replica Method

Maps of SNR are formed from the pseudo multiple replica method by first forming an image noise map. For each pixel the standard deviation in either the real or imaginary component of the complex image is found from the stack of image replicas. The SNR is then given by the magnitude of the image in the original reconstructed image, that is, that without additional noise added, divided by the value of the noise standard deviation for that pixel. We use the real component of the image because the image is completely real after reconstruction so as to avoid magnitude-related noise bias in low-SNR regions. Note that the image

noise is always correctly measured, without noise bias, from the complex data. The SNR map will always have itself the SNR of the acquired image from which the signal component of SNR is taken whereas the SNR of the image noise map may be made as high as desired by increasing the number of pseudo replicas reconstructed and is limited only by total available computation time.

g-Factor Maps From the Pseudo Multiple Replica Method

g-Factor maps are generally created directly from the reconstruction matrix as specified in Pruessmann et al. (2). To ensure the general applicability of the pseudo multiple replica method, a procedure is required for determining the *g*-factor that does not require acquisition of a fully sampled reference image to provide the image noise standard deviation for an unaccelerated acquisition in the expression for the *g*-factor in Equation [5] (where R is the acceleration factor).

Again taking advantage of the linearity of the reconstruction, the pseudo multiple replica method is applied to noise-only data. The unaccelerated image noise may be found by reconstructing a synthetic noise-only fully sampled *k*-space (i.e., the data has the full matrix size of the final image) instead of an acquired unaccelerated "image *k*-space". Repeated reconstruction of multiple replicas of noise-only *k*-space data produces a stack of noise-only image replicas whose pixel noise standard deviation gives the proper value for an unaccelerated acquisition. Alternatively, a direct image-noise calculation for $R = 1$ may be used (7).

Care must be taken to find the optimal-SNR image for the unaccelerated case to correctly define the *g*-factor. For both SENSE and GRAPPA techniques, this is given by an FFT, correctly scaled for unity gain of noise, followed by an optimal complex coil-combination described by Roemer et al. (15). The Roemer-optimum image is formed by the inclusion of the noise covariance matrix into the optimal coil-combination $\hat{\mathbf{C}}$ which appears in the GRAPPA matrix-reconstruction (Eq. [9]) as described in Robson et al. (9).

g-Factor maps are then found from the ratio of the noise standard deviation maps for an accelerated and an unaccelerated acquisition (Eq. [5]).

The procedure for measuring the noise covariance matrix and for performing the pseudo multiple replica measurement of the SNR and *g*-factor is described in Figure 1.

Pseudo Multiple Replica Method With Self-calibrated Approaches

The pseudo multiple replica technique relies on the image reconstruction being identical for each replica in order that fluctuations in the NMR signal are correctly translated into variance in the image domain. For "externally-calibrated" techniques, this condition is met. Conventionally, SENSE techniques use coil sensitivities obtained from a separate calibration image and are therefore externally calibrated. However, GRAPPA techniques are most often self-calibrating, finding the reconstruction weights from the acquired *k*-space itself (i.e. from the Auto-Calibrating-Signal lines). It is possible to implement an externally calibrated GRAPPA-reconstruction by using weights calculated from a separate equivalent *k*-space acquisition. In the case of self-calibrated techniques, it is important to use the same reconstruction for each replica in the pseudo multiple replica method. For SENSE techniques this requires the use of the same coil sensitivities for each replica. For GRAPPA techniques the same transfer matrix (or set of reconstruction weights) must be used as calculated for reconstructing the original accelerated image without pseudo-noise added (rather than using new weights calculated from synthetic noise-enhanced ACS in each replica).

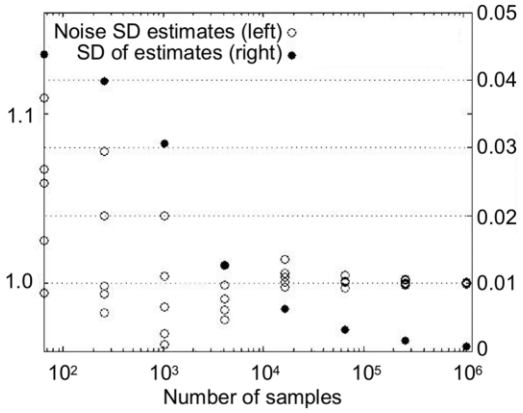

FIG. 2. Plot of the standard deviation (closed circles) of repeated (five) estimates of the noise-SD (open circles) of separate unity-variance Gaussian-distributed noise data of varying number of samples. For a single estimate of the noise-SD to have a standard deviation less than 1% of the true value (here 0.01), the noise data must comprise greater than approximately 10^4 samples.

METHODS

Pre-Scan Noise Measurement and Scaling

The required number of noise samples which must be taken to correctly measure the noise covariance matrix has been determined by calculating the SD of Gaussian distributed random noise records of various lengths N, which each have unit variance. This was repeated five times each for different values of N between 64 and 10^6. The SD of the five estimates for each N is plotted in Figure 2 showing that for a measurement of noise SD to be accurate to within 2% N must be greater than approximately 2000 and within 1% greater than approximately 8000 (following a $1/\sqrt{N}$ pattern). These values can be achieved by using image matrices of 64×64 and 128×128, respectively.

It was confirmed that digitization error was not important by observing a Gaussian character in a histogram plot of both the real and imaginary components of the noise received in each of the elements of the coil array with no NMR signal present. Twenty-one bins were used over the observed range of the noise.

It was assumed throughout that the noise is white in character, having equal power at all frequencies. Kellman and McVeigh describe the prescan noise measurement in greater detail (7).

Experiments

The pseudo multiple replica SNR measurement was validated with images of the manufacturer's standard spheri-

cal phantom. Pseudo multiple replica SNR and *g*-factor measurements were compared with gold-standard actual multiple replica SNR and *g*-factor measurements from 128 separately acquired 2D slice images and also compared with the direct SNR method (7,9). Both SENSE and GRAPPA methods were investigated for various acceleration factors with undersampling in one dimension.

2D acceleration with variable density *k*-space traversal was then investigated in phantoms where it is possible to validate the pseudo multiple replica method against the gold standard actual multiple replica method but not against a direct calculation.

The pseudo multiple replica method was then applied in vivo after obtaining written informed consent with approval of our institutional review board. First, in the brain, 1-D acceleration was used allowing the pseudo multiple replica method to be verified by a direct image-noise calculation, noting that no actual replica method is feasible in vivo. Finally, a 3D volumetric image of the abdomen was obtained using 2D acceleration, a variable density *k*-space trajectory and self-calibration. A clinical prescription was chosen which requires parallel imaging acceleration to acquire data in a single 22-s breath-hold demonstrating the pseudo multiple replica technique in a case for which no other method exists for calculating SNR and *g*-factor.

Pseudo multiple replica calculations used 128 image replicas throughout. The estimate of SNR and *g*-factor becomes increasingly accurate as the number of replicas is increased, thus the optimal choice of the number of replicas is somewhat arbitrary and depends on the desired accuracy and total computation time available. Using approximately 100 replicas gives an adequate accuracy of ~10% according to a $1/\sqrt{N}$ scaling relationship.

All data were acquired on a 1.5 Tesla (T) Excite-HDx whole-body scanner, (GE Healthcare, Waukesha, WI) using an 8-channel head coil array except the abdomen image which used an 8-channel body array. In the phantom and the brain images *k*-space data were acquired fully sampled and later decimated by removing some acquired phase-encoded lines from the data set to mimic accelerated acquisitions of various net reduction factors and *k*-space sampling patterns. Noise data were acquired from an equivalent separate single image with the amplitude of RF pulses set to zero and without changing transceiver settings, giving greater than 4096 data points, which was sufficient to calculate the noise covariance matrix.

An axial 2D slice of the phantom was acquired using a fast gradient recalled echo pulse sequence; imaging parameters included: matrix size of 64 × 64, field of view of 20 cm, slice thickness of 1 mm, acquisition bandwidth of ± 15.36 kHz, flip angle of 10°. 128 replicas of the same slice were acquired consecutively in a single experiment. *k*-Space data from the first replica acquisition were used with the direct SNR method and the pseudo multiple replica method. The chosen imaging parameters for the phantom experiment resulted in an image SNR of approximately 40 for a fully sampled image, which is sufficiently low that noise dominates shot-to-shot variation in the scanner in the determination of SNR from the actual multiple replicas (6). For a selection of pixels, pixel intensity in each replica was plotted against replica number (not shown) to confirm that no temporal drift was present in the actual multiple replica data.

An axial 2D slice of the brain was acquired using a T_1-weighted spin-echo pulse sequence; imaging parameters included: matrix size of 256 × 256, field of view of 22 cm, slice thickness of 5 mm, acquisition bandwidth of ± 15.36 kHz, TR/TE of 500/20 ms.

A coronal 3D volume of the abdomen was acquired with a T_1-weighted fast gradient recalled echo pulse sequence; imaging parameters included: in-plane matrix size of 200 × 200, with 80 3-mm slices, field of view of 36 cm, frequency-encode direction superior-inferior, acquisition bandwidth of ± 62.5 kHz, TR/TE of 3.9/1.7 ms, and flip angle 15°.

In-house implementations of an iterative conjugate-gradient generalized SENSE image reconstruction and a complex-combined GRAPPA method with conventional convolution-like *k*-space reconstruction (9) were used for the multiple replica images. In-house implementations were also used for the direct matrix-inverse generalized SENSE reconstruction and the direct complex-GRAPPA matrix-reconstruction (9). All image reconstruction and image replica analysis was performed using Matlab (The MathWorks, Natick, MA) and run on a standard PC with a Pentium IV 2.8 GHz CPU and 512 MB of RAM. The computation time required to generate SNR and *g*-factor maps is dominated by the reconstruction of the accelerated image replicas (the generation of pseudo noise, the formation of unaccelerated image replicas, and finding the final image noise standard deviation are all relatively rapid). Computation times varied according to the size of the image matrices being handled and reconstruction type; they were generally rather long, ranging from a few minutes for 128 conventional GRAPPA replicas with a matrix size of 64 × 64 to approximately 24 hr for 128 replicas of a CG-generalized SENSE reconstruction with a matrix size of 200 × 200 × 80. However, the Matlab code used in this work had not been optimized for speed, and significant reductions in computation time are likely to be possible.

g-Factor maps for the gold-standard actual multiple replica method (in the phantom) were formed by dividing the image-noise SD-maps calculated from the stack of actual accelerated image replicas by the image-noise SD-map calculated from the stack of actual optimal-SNR unaccelerated image replicas. It was confirmed that the image-noise SD-map calculated from the unaccelerated actual multiple replicas and the SD-map calculated using "pseudo fully sampled" noise and the pseudo multiple replica method were equivalent (not shown). Unaccelerated image-noise maps for the pseudo replica method used "pseudo fully sampled" noise throughout.

In all cases, for both SENSE and GRAPPA methods coil sensitivities were calculated from the fully sampled center of *k*-space which is filtered by a Kaiser-Bessel window with $\beta = 2$. In all cases except in the phantom for an outer reduction factor of 3 the undersampled *k*-space had a variable density sampling pattern.

RESULTS

Figure 3 shows the SNR-scaled images (intensity ≡ units of SNR) and *g*-factor maps for the 2D slice through the

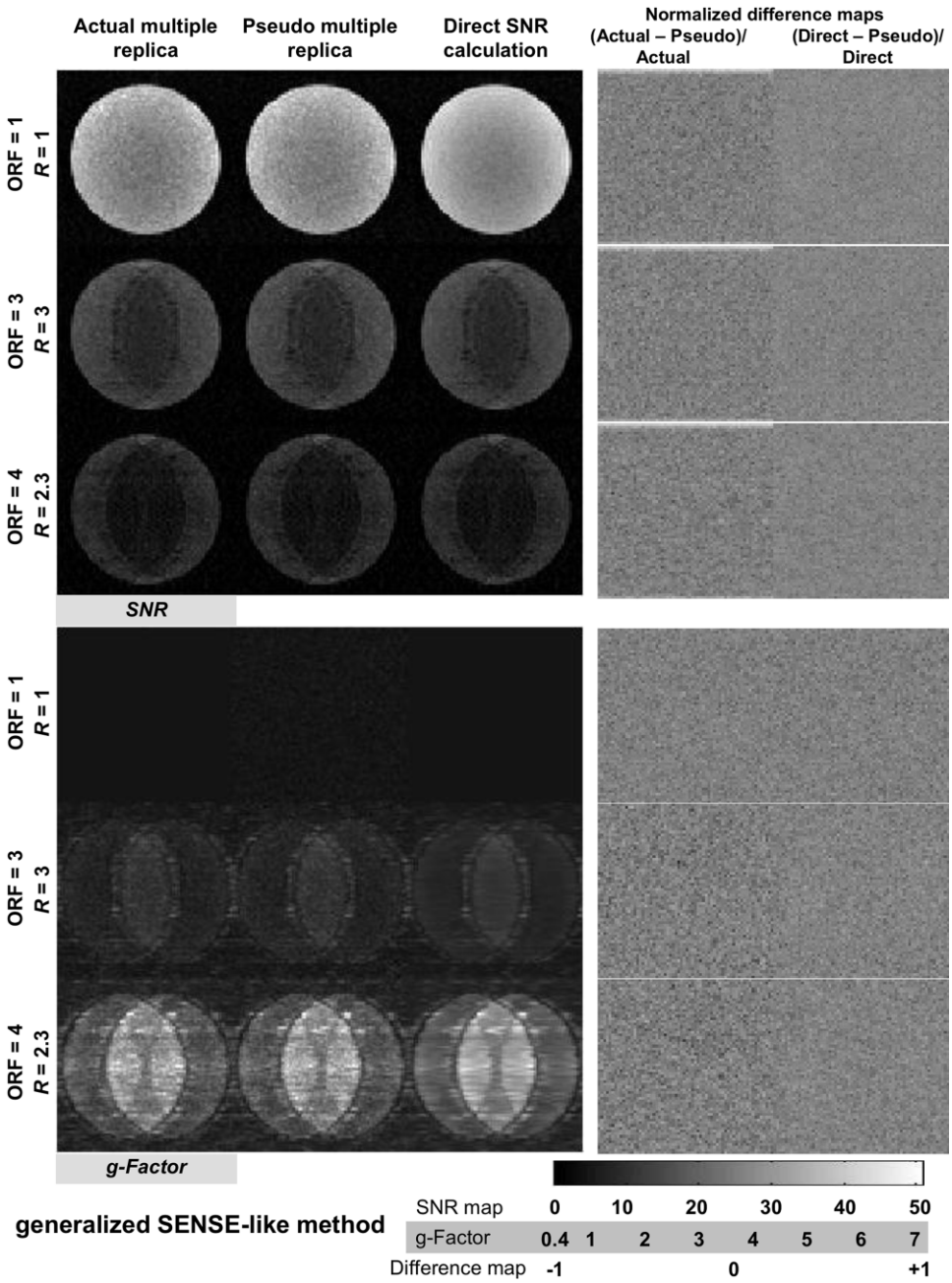

FIG. 3. SNR-scaled images and *g*-factor maps (three leftmost columns, SNR top, *g*-factor bottom) for various acceleration factors (ORF shown at left) using generalized SENSE reconstruction. There is excellent agreement between all methods: (i) actual multiple replica, (ii) pseudo multiple replica, and (iii) direct calculation. Iterative CG reconstruction is used for the multiple replica methods and matrix-inversion for the direct SNR method. Difference maps (two rightmost columns) for each acceleration between methods show negligible residual structure between all methods. (Phase-encoding/acceleration direction is left–right.)

phantom reconstructed using a SENSE image reconstruction. Measurements have been made using three methods: (i) actual multiple replica method, (ii) pseudo multiple replica method, and (iii) direct SNR method. SNR maps are shown for: (a) fully sampled image, (b) threefold regularly undersampled, and (c) variable-density undersampling with an outer reduction factor (ORF) of 4 and dense fully sampled center of 16 lines giving total acceleration factor $R = 2.3$. Difference maps between the pseudo multiple replica measurement and gold standard methods are shown for both SNR and *g*-factor maps. Difference maps are normalized to the gold-standard measurement. Figure 4 shows equivalent images using a GRAPPA image reconstruction. Interestingly, in the *g*-factor maps for the GRAPPA image reconstruction shown in Figure 4 there are localized regions in which the *g*-factor is less than one. This is a surprising feature which is discussed further below.

There is excellent agreement between the SNR and *g*-factor maps calculated with all methods and for all accelerations both in spatial distribution and in the overall scaling of SNR and *g*-factor values. The difference maps show there is no residual differential structure in the SNR or *g*-factor maps between methods. Computations of the mean value in the difference maps inside a mask of the phantom show that systematic error in the SNR and *g*-factor maps from the pseudo multiple replica method are always within 2% of the gold standard measurement. These small global errors are likely due to small inaccuracy in the measurement of the noise covariance matrix

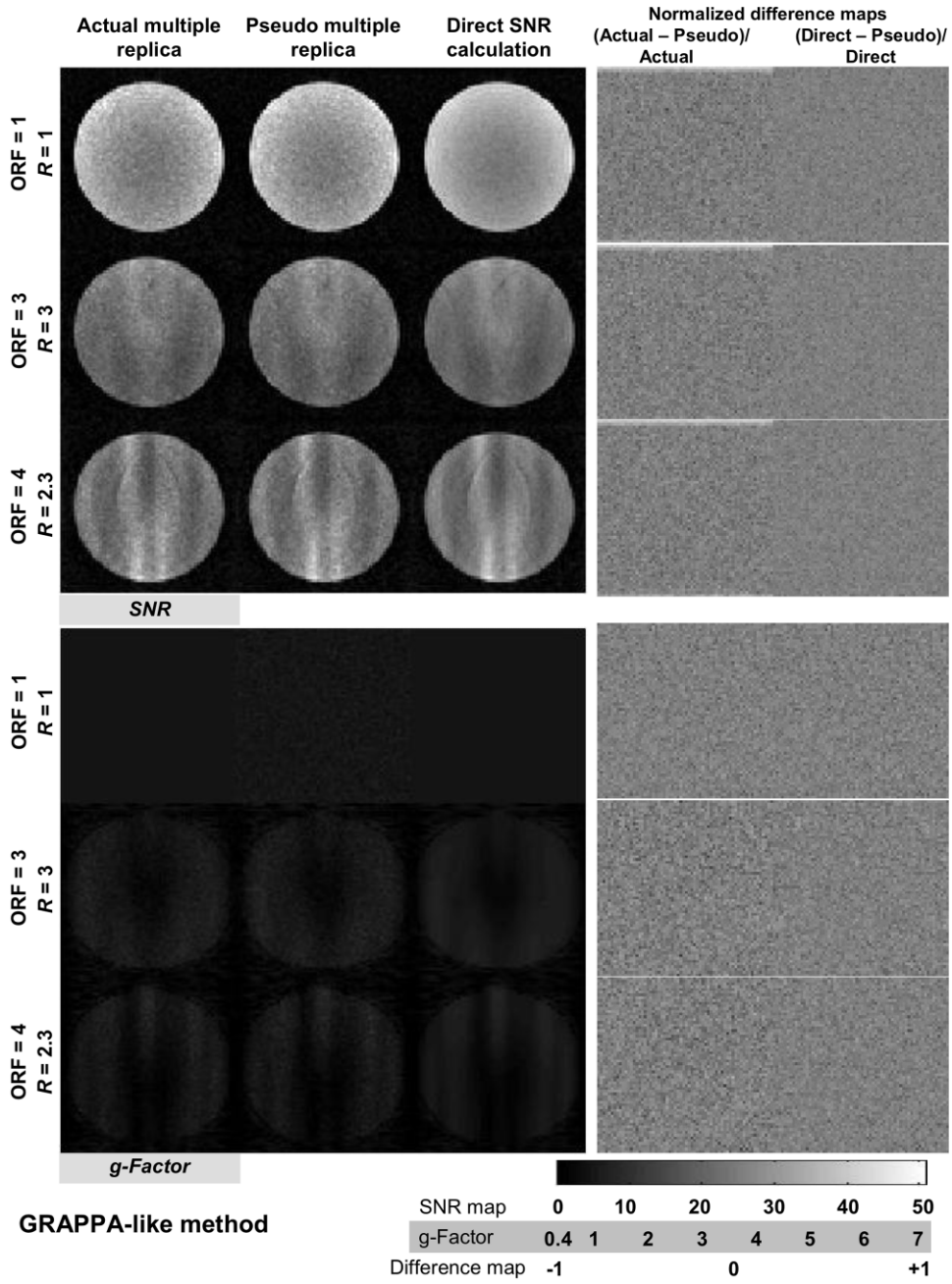

FIG. 4. SNR-scaled images and *g*-factor maps (three leftmost columns, SNR top, *g*-factor bottom) for various acceleration factors (ORF shown at left) using GRAPPA reconstruction. There is excellent agreement between all methods: (i) actual multiple replica (ii) pseudo multiple replica, and (iii) direct calculation. Conventional convolution-like reconstruction is used for the multiple replica methods and matrix-inversion for the direct SNR method; both use SNR-optimal complex coil-combination. Difference maps (two rightmost columns) for each acceleration between methods show negligible residual structure between all methods. (Phase-encoding/acceleration direction is left–right.)

when comparing to actual multiple replica noise, or due to some small scaling difference that exists between the direct image reconstructions and the reconstruction methods used for the multiple replica measurements.

As discussed by Kellman and McVeigh (7) the noise in the direct SNR method is determined from more samples (64×64) of the noise in the noise covariance matrix than the number of replica images (128); therefore, the SNR and *g*-factor maps for the multiple replica methods appear noisier than those from the direct SNR method. The light bands at the edges of the FOV evident in the gold-standard multiple replica difference maps in Figures 3 and 4 are a consequence of a sharp roll-off to the top-hat frequency response of the digital receiver which is not replicated in the pseudo noise; this does not affect the noise in the bandwidth including the image.

Figure 5 shows SNR and *g*-factor maps for both a SENSE and a GRAPPA image reconstruction method. Data were undersampled with an ORF of 2 in two-dimensions and included a dense center of *k*-space of 8 lines in both dimensions giving a total reduction factor $R = 3.1$. Excellent agreement is observed between the pseudo multiple replica method and the gold standard actual multiple replica method. Mean values of the difference maps within the mask of the phantom show systematic differences in the SNR and *g*-factor maps between the pseudo and actual multiple replica methods of less than 2%. It is interesting to note that despite being applied to exactly the same data, the SENSE and GRAPPA reconstructions give very different patterns of SNR and *g*-factor, as also observed by Thunberg and Zetterberg (13).

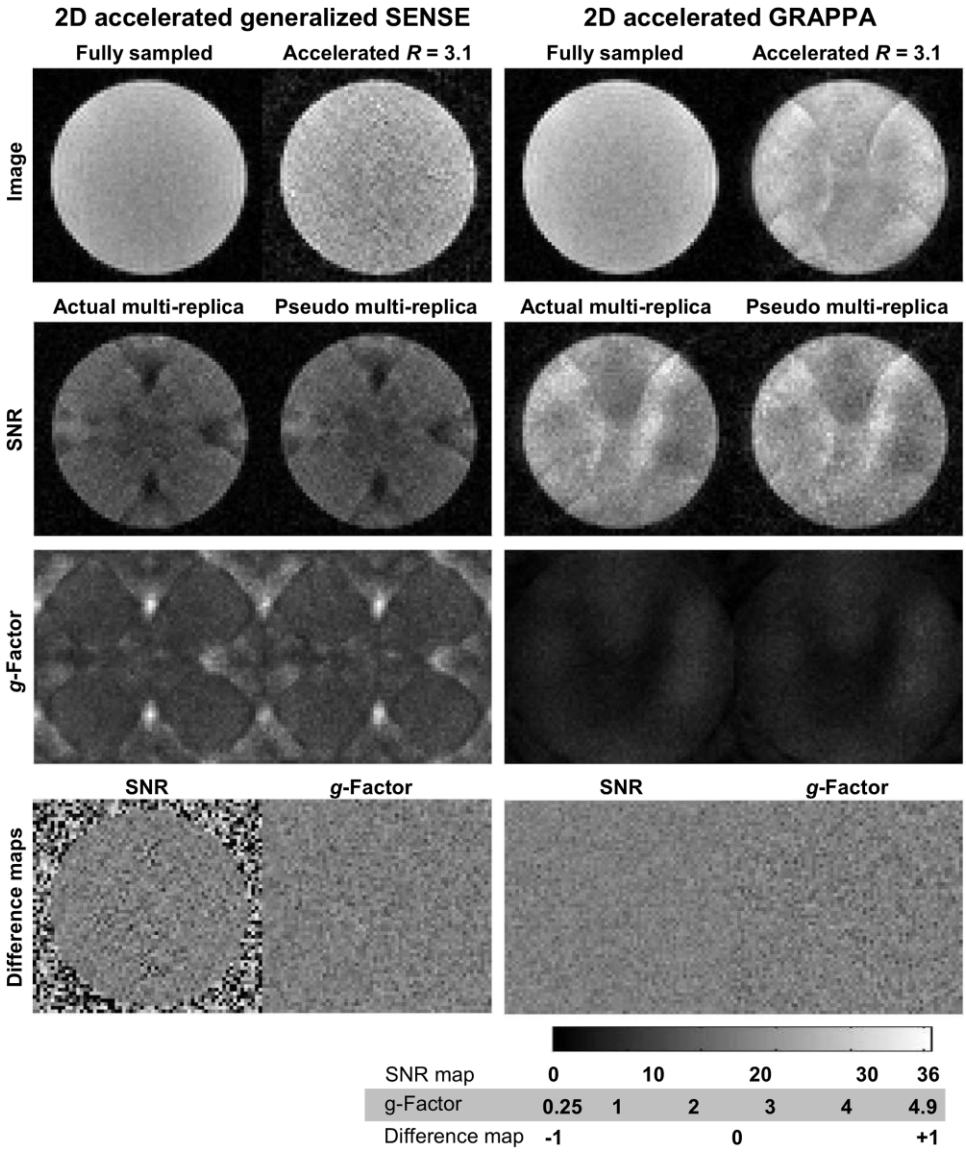

FIG. 5. SNR-scaled images and *g*-factor maps (SNR middle-top, *g*-factor middle-bottom) for 2D accelerated generalized SENSE and GRAPPA image reconstructions. A fully sampled and accelerated image is shown (top-left/top-right for each reconstruction method); an ORF of 2 in both dimensions was used with a dense center of 8 lines in each dimension giving $R = 3.1$ for the full matrix size of 64×64. CG-Generalized SENSE and convolution-like GRAPPA with complex-combination reconstructions were used. There is excellent agreement between pseudo multiple replica and actual multiple replica methods. Difference maps (bottom) between methods show negligible residual structure.

Figure 6 shows SNR and *g*-factor maps for the axial 2D brain image reconstructed using a SENSE and a GRAPPA technique undersampled with an ORF of 4 and including a dense fully sampled center of 32 lines giving a total acceleration $R = 2.9$. The SNR-scaled images and *g*-factor maps calculated using the pseudo multiple replica method are compared with those calculated using the direct SNR method and show excellent agreement (note that actual multiple replica measurement is not feasible due to subject motion limitations). Mean values of the difference maps within the mask of the brain show systematic differences in the SNR and *g*-factor maps between the pseudo multiple replica and direct SNR methods of less than 1%. The *g*-factor maps in the brain are familiar from those in the phantom where the overall geometry and the coil sensitivity distributions are similar.

Figure 7 shows SNR and *g*-factor maps for a coronal and axial-reformatted slice from the 3D volumetric image of the abdomen. Acquired data was undersampled with an ORF of 2 in both phase-encoded directions with a densely sampled center of 20 lines in each direction and a total acceleration factor $R = 2.63$. Image reconstruction used a generalized SENSE approach. No direct calculation of SNR and *g*-factor is computationally feasible with this *k*-space trajectory, because the reconstruction matrix was approximately 6 Gb (for a matrix size of 200×80 being undersampled by $R = 2.63$ and with 8 coils, see "Limitations of Conventional Noise Analysis" in the "Introduction" section); nor is an actual multiple replica method feasible in vivo.

DISCUSSION

g-Factor Less Than Unity for GRAPPA

It was noted in the Results section that a *g*-factor less than 1 is found when using a GRAPPA reconstruction. It is well established that a *g*-factor less than one is not possible for SENSE reconstructions that use a matrix inverse of the entire under-sampled *k*-space data (2). Any image recon-

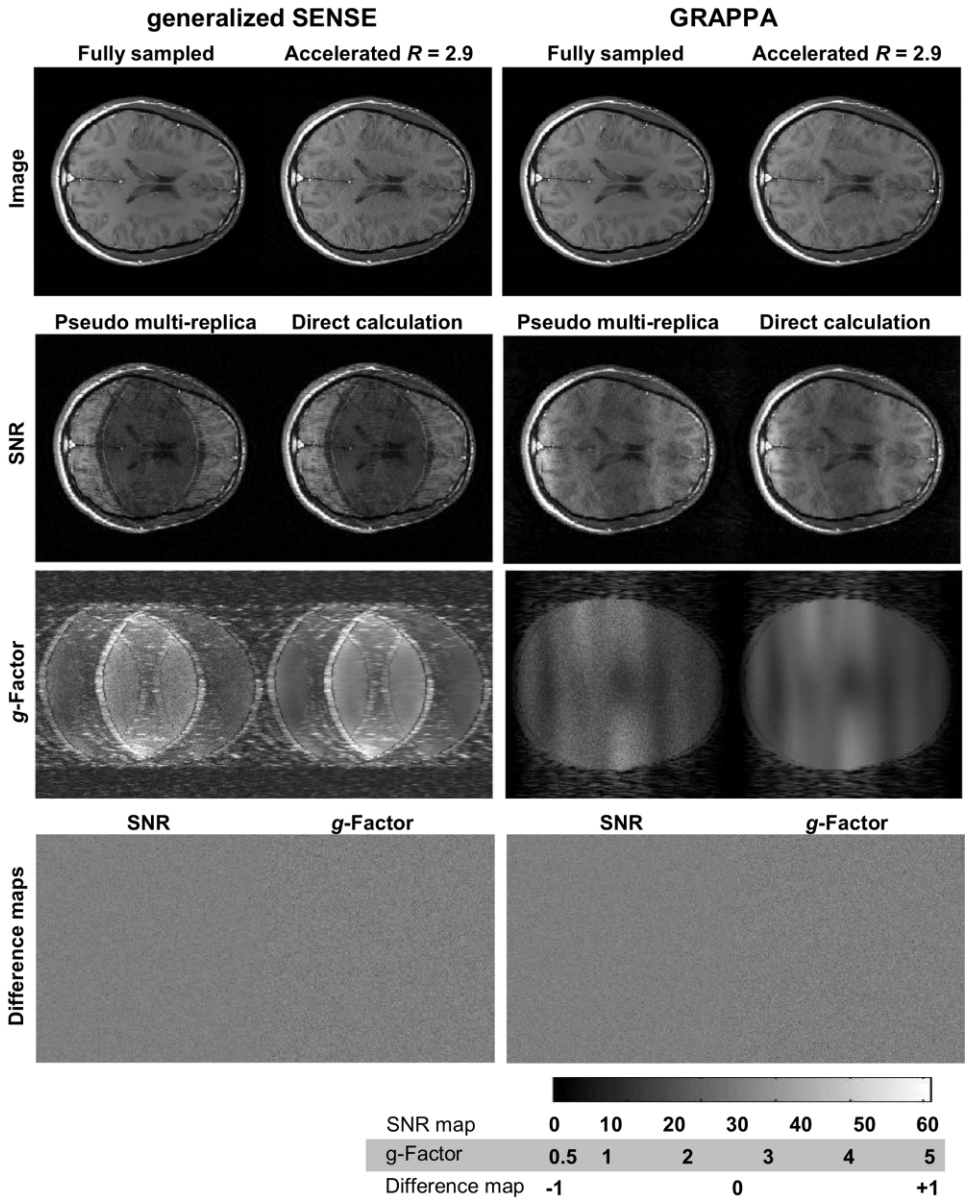

FIG. 6. SNR-scaled images and *g*-factor maps (SNR middle-top, *g*-factor middle-bottom) in vivo for generalized SENSE and GRAPPA image reconstructions. A fully sampled and accelerated image is shown (top-left/top-right for each reconstruction method); an ORF of 4 was used with a dense center of 32 lines giving $R = 2.9$ for the full matrix size of 256×256. CG-Generalized SENSE and convolution-like GRAPPA with complex-combination reconstructions were used with the pseudo multiple replica method; matrix-inverse generalized SENSE and full matrix GRAPPA image reconstruction was used for the direct method. There is excellent agreement between pseudo multiple replica and direct calculation methods. Difference maps (bottom) between methods show negligible residual structure.

struction (including modifications to SENSE techniques) may include explicitly some degree of numerical regularization to improve the apparent SNR and in such cases a *g*-factor less than unity may be found (24). We infer from the observation of $g < 1$ that our implementation of the GRAPPA technique includes some implicit conditioning of the noise. This has been observed and discussed in Robson et al. (9). The agreement of a direct calculation of *g*-factor and an actual multiple replica method indicates that this observation of $g < 1$ is a genuine finding. Such inherent conditioning is likely to stem from calculation of the weighting factors for fitting missing lines in *k*-space on a least-squares basis. Indeed, in the related SMASH reconstruction technique (1), the fitting process is explicitly approximate.

Pseudo Multiple Replica

The pseudo multiple replica method has been shown to be an accurate method of quantifying the image noise for both SENSE and GRAPPA techniques when compared with direct calculation of image noise and *g*-factor from the image noise matrices and to the gold-standard actual multiple replica values. Validation of the pseudo multiple replica method has been further demonstrated against the gold-standard actual replica method for a variable-density 2D-accelerated parallel imaging acquisition for which it is not feasible to calculate image noise directly due to the extremely large reconstruction matrix required for the direct calculation of image noise. While computation time for the pseudo multiple replica method is also long it requires repetitions of smaller computations and is therefore a preferred approach when direct approaches become unfeasible. The method has been used to produce maps of *g*-factor without requiring acquisition of an unaccelerated image permitting the method to be used in vivo when the need to acquire a lengthy unaccelerated image would be prohibitive (e.g., for volumetric image acquisition). Generation of *g*-factor maps in addition to SNR maps is benefi-

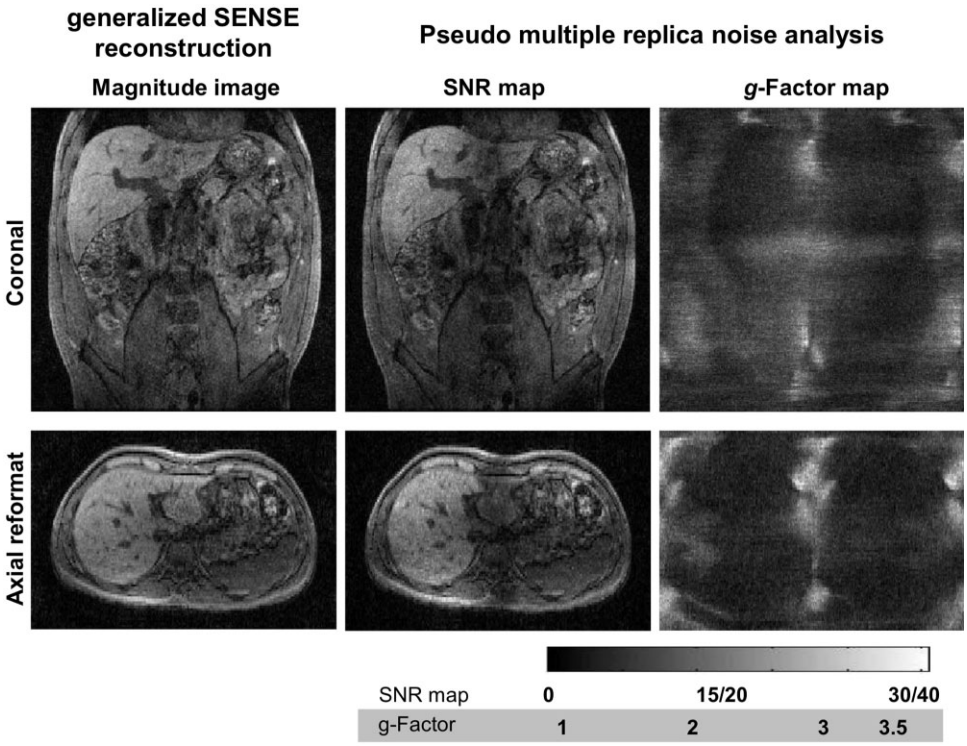

FIG. 7. SNR and *g*-factor maps calculated using the pseudo multiple replica method for slices from a 3D volumetric image acquired in vivo in a 22-s breathhold. A CG-generalized SENSE image reconstruction of data undersampled in two dimensions with ORF 2×2, a dense center of 20×20 lines and total acceleration $R = 2.63$ was used. The gray-scale maximum of 30/40 for SNR maps corresponds to coronal/axial orientations, respectively.

cial for assessing noise amplification because SNR maps include spatial variations due to the magnetization density as well as noise amplification. Furthermore, SNR maps include artifacts from the image reconstruction which should not be confused with localized regions of noise amplification. Additionally, the pseudo multiple replica technique is immune to the influence of instrumental drift and is, therefore, likely to out-perform acquisition of actual multiple replicas (4,5,21).

The noise prescan is both rapid and simple. For a typical receiver bandwidth of 60 kHz, the noise pre-scan could take as little as one sixth of a second given 10^4 samples required to measure the noise standard deviation to within 1%. Data acquisition simply requires opening the receiver without RF excitation, which easily may be incorporated into any imaging pulse sequence program.

In this work, we have made possible the comparison between the noise characteristics of different image reconstruction methods. In our implementations, it is apparent that GRAPPA techniques intrinsically control noise to a greater extent than SENSE techniques and demonstrate a more diffuse spatial variation of image noise as seen in their *g*-factor maps (13). In future studies, the pseudo multiple replica method will allow comprehensive, quantitative comparison between reconstruction techniques for which direct image noise calculations may not be available or may be computationally intractable. For example, in Figure 3, it is interesting to note that a lower total acceleration of $R = 2.3$ displays higher *g*-factor values and lower SNR due to the variable density of its *k*-space trajectory with ORF of 4 when compared with equivalent values for the regularly undersampled threefold acceleration; similar investigation of variable density trajectories where direct calculation of image noise is not computationally feasible will be possible.

Furthermore, because the pseudo replica method brackets the entire image acquisition and reconstruction process inserting random noise at the beginning and computing image noise in the final step, it is possible with this method to analyze the effect of image processing steps, for example, an explicit noise conditioning step, or the stopping condition chosen in iterative approaches.

Computation time is the principal drawback to the pseudo multiple replica method which may preclude routine implementation of SNR analysis. The lengthy image postprocessing time may be drastically reduced by implementing the analysis with optimized C-programs run on a faster dedicated computer. Furthermore, reconstruction of separate image replicas may be trivially parallelized on cluster or multi-core architectures. However, an important application of the SNR and *g*-factor analysis proposed here will be in developing new parallel imaging techniques and designing clinical imaging protocols—cases in which computation time may not be a primary constraint.

CONCLUSION

The pseudo multiple replica image noise measurement outlined here is a simple, robust and accurate method for the quantification of SNR and *g*-factor for all parallel imaging techniques which use a linear image reconstruction algorithm, encompassing the majority of clinical parallel imaging applications. This allows noise analysis for reconstructions that do not permit direct calculation of image noise. This approach will provide a useful tool for objective comparison between the in vivo-performance of parallel imaging methods being universally applicable with any signal acquisition schemes, *k*-space sampling schemes or trajectories, image reconstruction methods, image processing, or regularization techniques, hopefully guiding

choices as to which parallel imaging approaches are most appropriate for different clinical applications.

ACKNOWLEDGMENTS

We thank Dr. Peter Kellman for helpful discussions. C.A. McKenzie holds the Canada Research Chair in Parallel Magnetic Resonance Imaging at the University of Western Ontario. This research was undertaken, in part, thanks to funding from the Canada Research Chairs Program.

REFERENCES

1. Sodickson DK, Manning WJ. Simultaneous acquisition of spatial harmonics (SMASH): fast imaging with radiofrequency coil arrays. Magn Reson Med 1997;38:591–603.
2. Pruessmann KP, Weiger M, Scheidegger MB, Boesiger P. SENSE: sensitivity encoding for fast MRI. Magn Reson Med 1999;42:952–962.
3. Griswold MA, Jakob PM, Heidemann RM, Nittka M, Jellus V, Wang J, Kiefer B, Haase A. Generalized Autocalibrating Partially Parallel Acquisitions (GRAPPA). Magn Reson Med 2002;47:1202–1210.
4. Reeder SB, Wintersperger BJ, Dietrich O, Lanz T, Greiser A, Reiser MF, Glazer GM, Schoenberg SO. Practical approaches to the evaluation of signal-to-noise ratio performance with parallel imaging: application with cardiac imaging and a 32-channel cardiac coil. Magn Reson Med 2005;54:748–754.
5. Dietrich O, Raya JG, Reeder SB, Reiser MF, Schoenberg SO. Measurement of signal-to-noise ratios in MR images: influence of multichannel coils, parallel imaging, and reconstruction filters. J Magn Reson Imaging 2007;26:375–385.
6. Sodickson DK, Griswold MA, Jakob PM, Edelman RR, Manning WJ. Signal-to-noise ratio and signal-to-noise efficiency in SMASH imaging. Magn Reson Med 1999;41:1009–1022.
7. Kellman P, McVeigh ER. Image reconstruction in SNR units: a general method for SNR measurement. Magn Reson Med 2005;54:1439–1447.
8. Pruessmann KP, Weiger M, Börnert P, Boesiger P. Advances in sensitivity encoding with arbitrary *k*-space trajectories. Magn Reson Med 2001;46:638–651.
9. Robson PM, Grant AK, Madhuranthakam AJ, Lattanzi R, Sodickson DK, McKenzie CA. Quantification of SNR and g-factor for parallel MRI: Universal application to image-based and k-space-based image reconstructions. In: Proceedings of 16th Annual Meeting of ISMRM, Toronto, Canada, 2008. p. 1295.
10. Efron B. Bootstrap methods: another look at the Jackknife. Ann Statistics 1979;7:1–26.
11. Jones DK. The effect of gradient sampling schemes on measures derived from diffusion tensor MRI: A Monte Carlo study. Magn Reson Med 2004;51:807–815.
12. Steger TR, White RA, Jackson EF. Input parameter sensitivity analysis and comparison of quantification models for continuous arterial spin labeling. Magn Reson Med 2005;53:895–903.
13. Thunberg P, Zetterberg P. Noise distribution in SENSE- and GRAPPA-reconstructed images: a computer simulation study. Magn Reson Imaging 2007;25:1089–1094.
14. Riffe MJ, Blaimer M, Barkauskas KJ, Duerk JL, Griswold MA. SNR Estimation in fast dynamic imaging using bootstrapped statistics. In: Proceedings of the 15th Annual Meeting of ISMRM, Berlin, Germany, 2007. p. 1879.
15. Roemer PB, Edelstein WA, Hayes CE, Souza SP, Mueller OM. The NMR phased array. Magn Reson Med 1990;16:192–225.
16. Sodickson DK, McKenzie CA. A generalized approach to parallel magnetic resonance imaging. Med Phys 2001;28:1629–1643.
17. Jakob PM, Griswold MA, Edelman RR, Sodickson DK. AUTO-SMASH: a self-calibrating technique for SMASH imaging. MAGMA 1998;7:42–54.
18. Wang Z, Wang J, Detre JA. Improved data reconstruction method for GRAPPA. Magn Reson Med 2005;54:738–742.
19. Weiger M, Pruessmann KP, Boesiger P. 2D SENSE for faster 3D MRI. MAGMA 2002;14:10–19.
20. Heidemann RM, Griswold MA, Seiberlich N, Kruger G, Kannengiesser SAR, Kiefer B, Wiggins G, Wald LL, Jakob PM. Direct parallel image reconstructions for spiral trajectories using GRAPPA. Magn Reson Med 2006;56:317–326.
21. NEMA Standards Publication MS 1-2001. Determination of signal-to-noise ratio (SNR) in diagnostic magnetic resonance imaging. Rosslyn, VA: National Electrical Manufacturers Association; 2001.
22. Constantinides CD, Atalar E, McVeigh ER. Signal-to-noise measurements in magnitude images from NMR phased arrays. Magn Reson Med 1997;38:852–857.
23. Kellman P, McVeigh ER. Image reconstruction in SNR units: a general method for SNR measurement. Magn Reson Med 2005;54:1439–1447. Erratum in: Magn Reson Med 2007;58:211–212.
24. Lin F-H, Kwong KK, Belliveau JW, Wald LL. Parallel imaging reconstruction using automatic regularization. Magn Reson Med 2004;51:559–567.